JOURNAL OF EARTHQUAKE ENGINEERING
2018, VOL. 22, NO. S2, 5–27
https://doi.org/10.1080/13632469.2018.1540372

Taylor & Francis
Taylor & Francis Group

Check for updates

Seismic Reliability of Code-Conforming Italian Buildings

Iunio Iervolino [a], Andrea Spillatura [b], and Paolo Bazzurro [b]

[a]Dipartimento di Strutture per l'Ingegneria e l'Architettura, Università degli Studi di Napoli Federico II, Naples, Italy; [b]Istituto Universitario di Studi Superiori di Pavia (IUSS), Pavia, Italy

ABSTRACT

This paper presents and discusses some research results related to the seismic failure risk of standard, residential and industrial, buildings designed for *damage*, and *life-safety* according to the Italian seismic code, which is somewhat similar to Eurocode 8. The five considered structural typologies are as follows: masonry, cast-in-place reinforced concrete, precast reinforced concrete, steel, and base-isolated buildings. The archetype structures have been designed according to standard practice at three sites, representative of the seismic hazard across the country. Seismic risk is defined here as the annual rate of earthquakes able to cause structural failure in terms of *usability-preventing damage* and *global collapse*. For each structure, the failure rates have been evaluated in the framework of performance-based earthquake engineering, that is, via integration of site's probabilistic hazard and structural fragility. The former has been computed consistently with the official hazard model for Italy that is also used to define design actions in the code. The latter has been addressed via nonlinear dynamic analysis of three-dimensional numerical structural models. Results indicate that, generally, design procedures are such that seismic structural reliability tends to decrease with increasing seismic hazard of the building site, despite the homogeneous return period of exceedance of the design seismic ground-motion.

ARTICLE HISTORY
Received 22 May 2018
Accepted 20 October 2018

KEYWORDS
Performance-Based Earthquake Engineering; Risk; Failure; Damage; Collapse; Hazard

1. Introduction

The Italian building code, the *Norme Tecniche per le Costruzioni* (NTC hereafter), requires engineers to design earthquake-resistant structures in compliance with a number of predefined performance thresholds, or *limit states* [CS.LL.PP., 2008, 2018], for ground-motion intensities that have a specified exceedance probability (or an approximation of it) in a given time interval at the building site. Design is carried out so that the structure is expected to withstand, at the site of the construction, relatively rare ground-motion intensities, computed according to probabilistic seismic hazard analysis (PSHA) [e.g., Cornell, 1968; McGuire, 2004]. Design ground-motion intensities are those that are exceeded at the building site, on average, once in a number of years; i.e., the *return period* of exceedance, T_R in the following. For example, an ordinary structure designed for the *life-safety* limit state should withstand ground-motions with $T_R = 475$ years (i.e., probability of exceedance of 10% in 50 years).

CONTACT Iunio Iervolino iunio.iervolino@unina.it Dipartimento di Strutture per l'Ingegneria e l'Architettura, Università degli Studi di Napoli Federico II, Naples, Italy

Color versions of one or more of the figures in the article can be found online at www.tandfonline.com/ueqe.

This article has been republished with minor changes. These changes do not impact the academic content of the article.
© 2018 Taylor & Francis Group, LLC

As in many modern seismic codes, while the design elastic seismic actions are probabilistically defined, the risk of failure of Italian code-conforming structures resulting from these design provisions is not explicitly controlled, and ultimately not known. Moreover, because design procedures may be different for different structural typologies or multiple design options may be available for the same structural type, the code does not explicitly warrant that different structures designed for the same site, or similar structures at different sites, have the same probability of failing the same performance target.

Insights about the seismic structural reliability (or risk) implied by design according to current standards are a starting point to understand the adequacy of the code and, eventually, to stimulate improvements, if needed. This was indeed the goal of a large national research program: the *RINTC—Rischio Implicito delle Strutture Progettate Secondo le NTC* project, which ran between 2015 and 2017 [RINTC Workgroup, 2018]; see Acknowledgments. For the purposes of the project, three[1] Italian sites were considered so as to span a wide range of seismic hazard levels within the country. The three sites are Milan (MI), Naples (NA), and L'Aquila (AQ), corresponding to low-, mid-, and high-hazard. Figure 1 (left) shows the site locations on the hazard map officially adopted by NTC, which reports the design peak ground acceleration (PGA) with $T_R = 475$ years on rock soil conditions. The life-safety-design PGA of the sites varies between 0.05 g for Milan and 0.26 g for L'Aquila.

Several buildings belonging to the five structural typologies mentioned above were designed for two local soil conditions, namely A- and C-type (defined according to NTC and Eurocode 8, or EC8, classification [C.E.N., 2004]) at the three sites: *unreinforced masonry (URM), cast-in-place reinforced concrete (RC), precast reinforced concrete (PRC), steel*, and *base-isolated (BI)*. The design was carried out to comply with two code-defined limit states, namely *damage* and *life-safety* (see Fig. 1, right, for

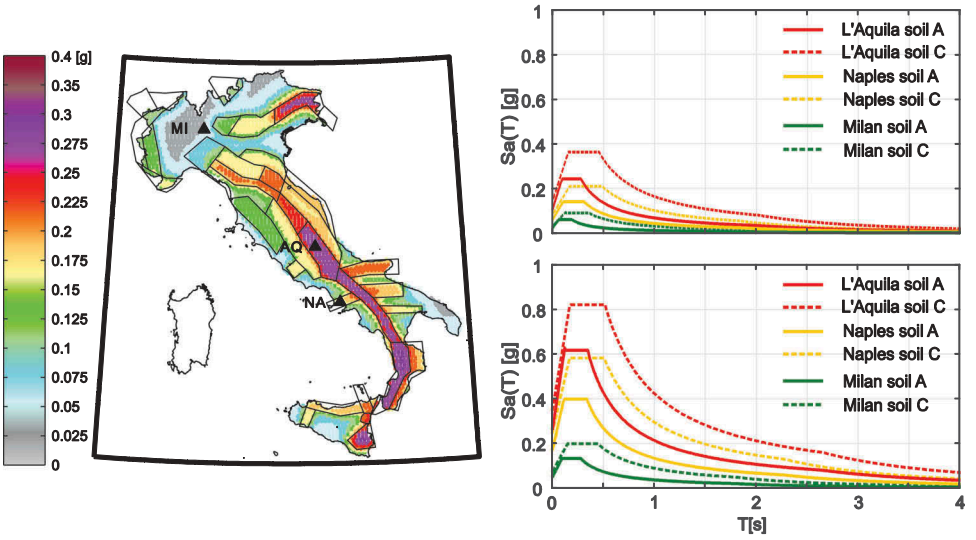

Figure 1. Left: Italian seismic source zones and official hazard map in terms of PGA with 475-year return period of exceedance on rock; right: design elastic spectra corresponding to 50-year (for damage limit state, top) and 475-year (for life-safety limit state, bottom) return periods at the considered sites (in the spectra, T is the natural vibration period).

the corresponding design spectra). Three-dimensional nonlinear structural models, generally based on lumped plasticity, were developed and their seismic performance was evaluated via *multi-stripe dynamic analysis* [Jalayer, 2003]. This approach provides a probabilistic characterization of the seismic response for a range of ground-motion intensities at the site of interest. The latter, coupled with the probabilistic seismic hazard that supported the definition of the design actions illustrated in Fig. 1 (right), allowed to calculate the seismic structural reliability, expressed in terms of annual failure rates.[2] These rates were evaluated with respect to two ad-hoc defined performance levels, namely *global collapse* and *usability-preventing damage*. The main source of uncertainty in structural response, for a given level of ground-motion intensity, is the one known as *record-to-record variability*. Additionally, the so-called model uncertainty (i.e., uncertainty in material properties, design options, and structural elements' constitutive relationships) was also accounted for in selected cases. This also applies to the soil–structure interaction (SSI).

The objective of this paper is to illustrate and discuss the main results of the RINTC project. To this aim, it is structured describing first the general methodology adopted to compute the seismic structural reliability. Then, the archetype structures and failure criteria are briefly recounted. Subsequently, a discussion about seismic hazard and ground-motion selection for nonlinear dynamic analysis is given. The article ends with the discussion of the resulting failure rates.

2. Methodology

All the considered structures are designed to comply with two code-specified limit states and, therefore, their seismic reliability is assessed for the two different performance conditions specified in the next section. For reliability computations, the *performance-based earthquake engineering* [Cornell and Krawinkler, 2000] framework was employed.

The failure rate λ_f is of interest for the reliability assessment because it is possible to show that if earthquakes occur according to a homogenous Poisson process (HPP), then also the counting process of earthquakes capable of causing failure is an HPP, characterized by the λ_f rate. Thus, the probability that the structure fails in any time interval, ΔT, can be computed as $1 - e^{-\lambda_f \cdot \Delta T}$.

For all the case-study buildings, independently of structural typology and limit state, the failure rates are obtained by integrating structural fragility and seismic hazard for the sites where the structures are located:

$$\lambda_f = \int_0^{+\infty} P[failure|IM = x] \cdot |d\lambda_{IM}(x)| \tag{1}$$

In Eq. (1), $\lambda_{IM}(x)$ is the annual rate of earthquakes causing the exceedance of an intensity measure (IM) equal to a specific value, $IM = x$, at the building site (from PSHA) and $P[failure|IM = x]$, $\forall x$ is the fragility of the structure. The term λ_{IM} has been evaluated for each site in terms of the 5% damped (pseudo)spectral acceleration at the fundamental period of the structure, $Sa(T_1)$ or simply Sa. The seismic hazard was computed considering the same source model adopted by NTC to define the seismic design actions (to follow).

In this study, the domain of the IM was discretized into ten values and the seismic response was assessed, for each of these IM values, via nonlinear dynamic analysis. At each of the 10 levels, 20 ground-motion records were selected, all featuring the same IM value. The sample of 20 response values collected in this way forms a so-called stripe, because, in a hypothetical plot of response versus IM, they are all aligned.

For each designed structure, the fragility was computed via nonlinear dynamic analysis using Eq. (2).

$$P[failure|IM = x_i] = \left\{1 - \Phi\left[\frac{log\left(edp_f\right) - \mu_{\log(\mathrm{EDP})|IM=x_i}}{\sigma_{\log(\mathrm{EDP})|IM=x_i}}\right]\right\}\left(1 - \frac{N_{\mathrm{col},IM=x_i}}{N_{\mathrm{tot},IM=x_i}}\right) + \frac{N_{\mathrm{col},IM=x_i}}{N_{\mathrm{tot},IM=x_i}} \tag{2}$$

In Eq. (2), EDP (i.e., the engineering demand parameter) represents the structural response measure (e.g., maximum inter-story drift) and edp_f is the structural capacity for the performance of interest. The quantities $\left\{\mu_{log(EDP)|IM=x_i}, \sigma_{log(EDP)|IM=x_i}\right\}$ are the mean and standard deviation of the logarithms of EDP when $IM = x_i,\ i = \{1, \ldots, 10\}$, while $\Phi(\cdot)$ is the cumulative Gaussian distribution function and $N_{col,IM=x_i}$ is the number of collapse cases (i.e., those reaching numerical instability according to the terminology of Shome and Cornell [2000]). Finally, $N_{tot,IM=x_i}$ is the number of ground-motion records, here 20, with $IM = x_i,\ i = \{1, \ldots, 10\}$.

Although Eq. (2) is the general framework, a nonparametric approach has been used in selected cases[3]; i.e., $P[failure|IM = x]$ has been empirically evaluated by counting the number of records for which failure has been observed, $N_{f,IM=x_i}$, as shown in Eq. (3).

$$P[failure|IM = x_i] = \frac{N_{f,IM=x_i}}{N_{tot,IM=x_i}} \tag{3}$$

As discussed in the following, the method to probabilistically evaluate structural response and, from it, the seismic fragility for a given limit state is the multi-stripe nonlinear dynamic analysis in which ground-motion input changes to reflect disaggregation of seismic hazard at each of the ten IM levels.[4]

3. Archetype Structures

The five types of buildings refer, as much as possible, to standard modern constructions and are widely representative of residential or industrial structures. Design refers to code prescriptions for ordinary constructions, requiring design for two limit states: damage and life-safety. The design procedures adopted are, to the extent possible, similar to those commonly adopted in professional engineering practice. According to the code, the damage limit state is not violated if the usability of the structure is preserved, while the life-safety limit state is not violated if the structure preserves part of the vertical-load bearing capacity and some (unspecified) capacity against further horizontal actions. Design requires structural verifications against the ground-motions consistent with the uniform-hazard spectrum (UHS) with 50- and 475-year exceedance return periods at the site for the damage and the life-safety limit states, respectively (see Fig. 1, right).[5]

The general characteristics of the structures considered here are very briefly summarized in the following, while the interested reader should refer to the cited papers for further details.

Cast-in-place RC: regular 3-, 6-, and 9-story (st) residential moment-resisting-frame (MRF) (bare frames or BFs, *pilotis* frames or PF, infilled frames or IF; Fig. 2) and nine-story shear wall (SW) structures designed via modal response spectrum analysis [Camata *et al.*, 2017; Ricci *et al.*, 2018]. All the RC structures were designed for a *behavior factor* equal to 3.9 (*low-ductility* class in NTC) and the BFs were considered as reference cases well studied in the literature.

URM: two- and three-story regular (reg.) and irregular (irr.) residential buildings (Fig. 3), with four different geometries,[6] designed with the *simple building* and *linear* or *nonlinear static analysis* (LSA) approaches [Camilletti *et al.*, 2017; Cattari *et al.*, 2018; Manzini *et al.*, 2018]. In case of LSA, the behavior factor was taken equal to 3.6.

PRC: one-story industrial buildings with two different plan geometries and two different heights with and without cladding panels (Fig. 4). The structures are all single-story one-bay frames. Bay span is equal to either 20 or 30 m, while the height is 6 or 9 m. The behavior factor for horizontal and vertical components of ground-motion was taken equal to 2.5 and 1.5, respectively [Ercolino *et al.*, 2017; Magliulo *et al.*, 2018]. The crane was also considered in design.

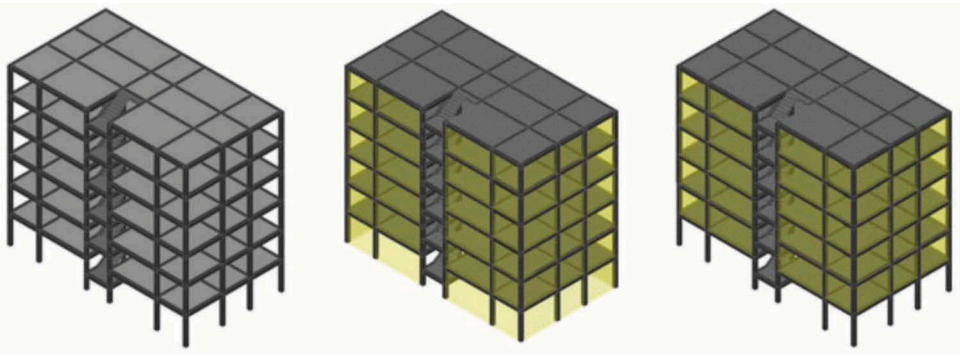

Figure 2. Example of six-story RC building structures: bare frame (left), infilled frame (center); pilotis frame (right).

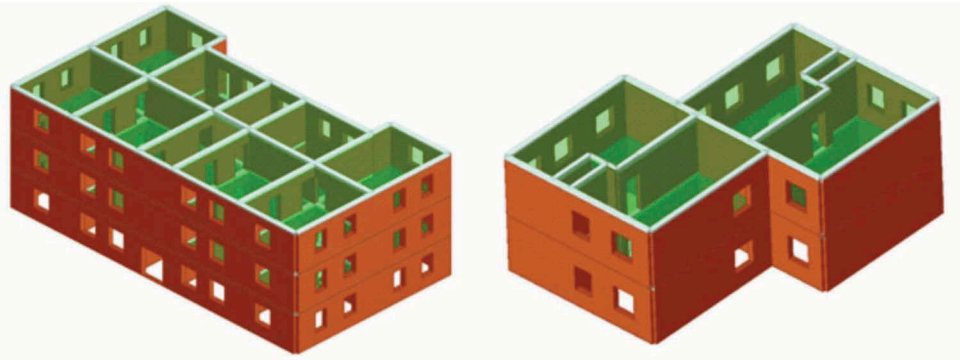

Figure 3. Example of regular three-story (left) and irregular two-story (right) URM building structures.

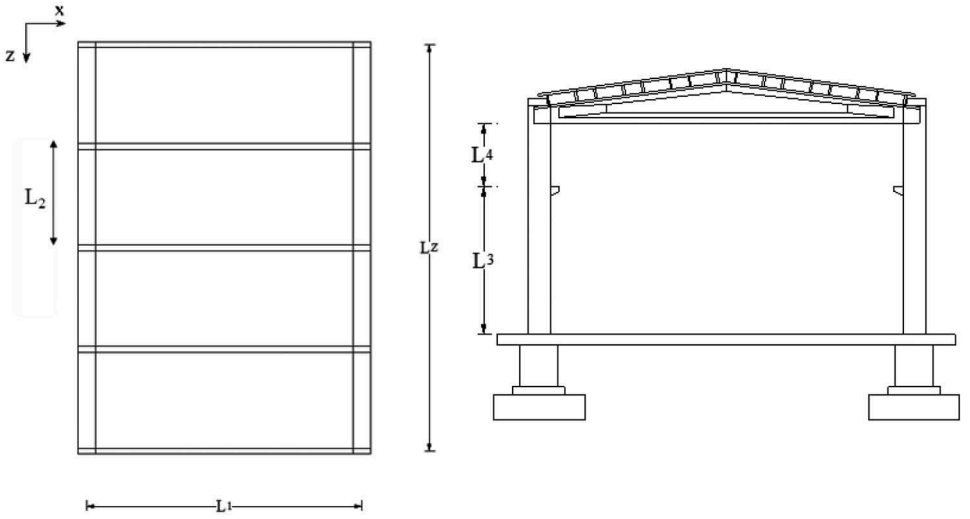

Figure 4. Example of precast industrial building. Left: plan view of structural elements; right: front view, including foundations.

Steel (S): one-story industrial buildings with two different plan geometries and two different heights modeled with and without cladding panels. The structures are all a single-story one-bay frames, with bracings in one direction only (Fig. 5). The design seismic actions both in horizontal and directions were obtained considering a behavior factor equal to 4.0 (for both MRF and frames with concentric braces in low-ductility class). The two geometries investigated are similar to those in the PRC case. The crane was also considered. Snow and wind loads specific to the considered sites were also considered in design [Scozzese *et al.*, 2017, 2018].

BI: six-story RC residential buildings with a base isolation system made of high-damping rubber bearings (HDRB), double-curvature friction pendulums, and hybrid

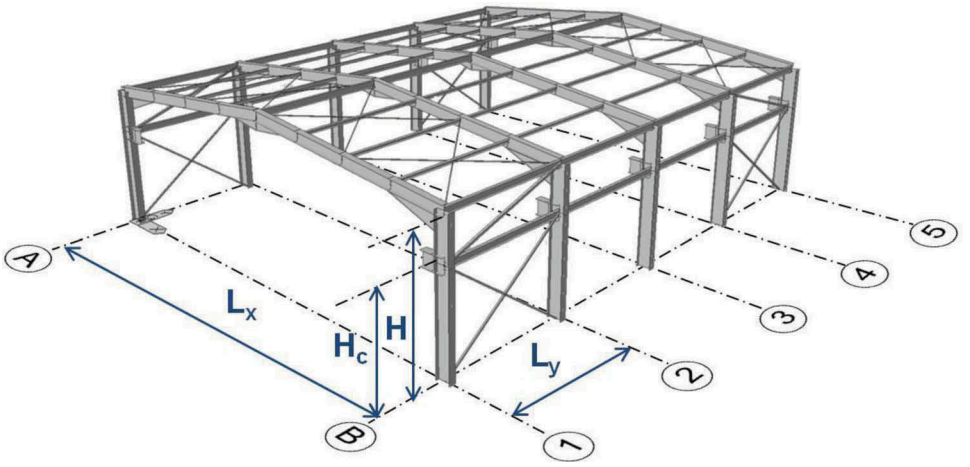

Figure 5. Example of steel industrial building.

(HDRB and sliders, HDRB+Sld) [Cardone *et al.*, 2017; Ragni *et al.*, 2018]. (Actually, NTC requires that the isolation system for ordinary constructions must be verified against ground-motion with 975-year return period of exceedance.) The behavior factor for the (isolated) RC superstructures is equal to 1.5.

Apart from these structures, some special cases were also considered. Although record-to-record variability of seismic response is the primary source of uncertainty in this study (i.e., the structural models are deterministic), the uncertainty in structural modeling (later labeled as Unc.) and in the design approach has been accounted for selected cases of each typology. For this task, the spatial stochastic dependence of *within-building* variability of material characteristics and nonlinear member properties was considered. However, the effect of factors, such as quality of construction or design errors, was neglected. The following list summarizes the considered modeling uncertainties for each structural typology [see Franchin *et al.*, 2017, 2018; for more detailed discussions].

- URM: masonry Young's modulus; masonry compressive and initial shear strength, failure thresholds.
- RC: concrete strength, steel yielding strength, concrete members parameters (stiffness, cyclic degradation, capping, and post-capping deformations).
- S: steel yielding strength, equivalent geometric imperfection in bracings.
- BI: friction coefficient in friction pendulums; shear modulus and rubber damping ratio in high-damping rubber bearings.

Moreover, the effect of SSI was also considered for the case of the nine-story RC buildings with SWs designed for a site in Naples with deformable soil conditions (soil C according to Eurocode 8). Further details on the SSI case studies can be found in RINTC Workgroup [2018], while Table 1 summarizes the case studies and the condition/sites for which they were designed.

4. Failure Criteria

The seismic performance of all the structures listed above was assessed by carrying out nonlinear dynamic analysis on three-dimensional computer models. All models are lumped plasticity (apart industrial steel buildings) and were analyzed with OPENSEES [Mazzoni *et al.*, 2006] except for the masonry structures that were analyzed using

Table 1. Designed structures per site and soil category.

Type	Soil	Milan	Naples	L'Aquila
RC	A	–	–	9-story (BF/PF/IF)
	C	3/6/9-story (BF/PF/IF)	3/6/9-story (BF/PF/IF), w/Unc.	3/6/9-story (BF/PF/IF), w/Unc.
		9-story SW	9-story SW (also w/SSI)	9-story SW
URM	A	2/3-story, reg.	2/3-story, reg./irr.	2/3-story, reg. w/Unc.
	C	2/3-story, reg.	2/3-story, reg./irr.	2/3-story, reg./irr.
PRC	A	1-story, 4 geometries	1-story, 4 geometries	1-story, 4 geometries
	C	1-story, 4 geometries	1-story, 4 geometries	1-story, 4 geometries
S	A	1-story, 4 geometries	1-story, 4 geometries	1-story, 4 geometries, w/Unc.
	C	1-story, 4 geometries	1-story, 4 geometries	1-story, 4 geometries, w/Unc.
BI	A	–	–	–
	C	–	6-story, HDRB/HDRB+Sld/DCFP	6-story, HDRB/HDRB+Sld/DCFP, w/Unc.

TREMURI [Lagomarsino *et al.*, 2013]; see the typology-specific papers referenced in the previous section for modeling details. All the analyses neglected the vertical components of ground-motion because a dedicated sensitivity analysis did not identify any significant change.

The failure criteria, for the two performance levels considered for the reliability assessments, were defined, to the extent possible, in a consistent manner across structural typologies. They were furthermore defined in terms of quantities whose values could be extracted from the results of the nonlinear dynamic analyses.

4.1. *Global Collapse*

In general, the global collapse criterion is based on the deformation capacity (the EDP is either the roof displacement or the inter-story drift ratio) corresponding to a certain level of strength deterioration, measured on the nonlinear static capacity curves of the structural models (Fig. 6). However, some exceptions and adjustments were needed for some specific cases (e.g., for steel structures).

For URM buildings, the collapse criteria were defined based on the value of the maximum inter-story drift of single-wall elements that corresponds to a 50% drop of the maximum base-shear from pushover analysis. For each structure, static pushover analysis was carried out under various load patterns in both horizontal directions and the minimum value emerging from them was defined as the collapse limit threshold. (Verification with some tests via nonlinear dynamic analysis leads to consider the EDP corresponding to 35% drop instead of 50%, in cases deformation capacity the deformation capacity from the analysis was found lower than that coming according to the static criterion.)

For RC buildings, the collapse criteria were defined based on the roof drift value corresponding to a 50% drop from the maximum base-shear computed via pushover analysis in each of the two horizontal directions.

For PRC buildings, two collapse criteria were considered. The first relates to global collapse, similarly to what was done for RC buildings, while the second accounts for local failure of the beam-to-column connections, which are critical elements for this kind of structures. Local failure was assumed to occur when the maximum shear strength is reached.

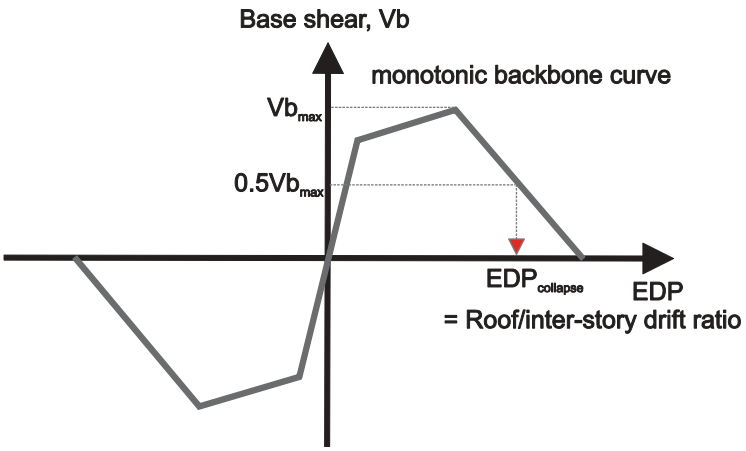

Figure 6. General definition for the global collapse failure criterion (RC, URM, PRC, and BI).

Since the prototype steel buildings have different load-resisting systems in the two horizontal directions, the collapse criteria were defined independently for each direction. A value of 10% inter-story drift was selected for the direction aligned with the moment-resisting frame system, whereas the failure in the concentrically-braced frame system was assumed to have been reached for a maximum strain range value of 4.9%. This range was defined as the difference between minimum and maximum strain responses measured at the cross-sections of brace members.

The collapse condition for BI reinforced concrete buildings was assumed to occur either if the superstructure fails or if the base isolation system fails. The superstructure failure criterion is analogous to the one used for the RC buildings, while the failure of the base isolation was defined based on the specific device's responses. Three different failure mechanisms were considered for HDRB: cavitation, buckling, and shear failure; see Ragni *et al.* [2018] for details.

For all the structural models in any dynamic analysis, the occurrence of global collapse was checked using the maximum demand-over-capacity ratio between the two directions.

4.2. *Usability-Preventing Damage*

The criteria for usability-preventing damage are based on a multi-criteria approach that considers the onset of any of the following three conditions:

(a) a widespread light damage condition: light damage in 50% of the main nonstructural elements (e.g., infills);
(b) a severe damage condition: at least one of the nonstructural elements reached a severe damage level leading to significant interruption of use;
(c) attainment of 95% of the maximum base-shear of the structure, Fig. 7.

For URM buildings, the criteria were defined as follows: (a) light-widespread damage in 50% of masonry walls (computed in terms of resisting area) in each direction; (b) at least one of masonry walls reached the drift limit corresponding to a certain level of strength deterioration (e.g., a 40% drop for shear failure) in the case of the phenomenological nonlinear beam or attainment of the toe-crushing condition in the case of the macroelement mechanical model; (c) the attainment of 95% of the maximum base-shear of the structure. It should be noted that the final threshold should be associated to a value of the base shear not lower than the 85% of the peak resistance. This lower bound is justified because URM buildings may show slight but widespread damage even for values of the base shear far from the peak value.

For RC and BI RC cases, the criteria were defined as follows: (a) light-widespread damage in 50% of masonry infills and partitions; (b) at least one of the masonry infills and partitions reached 50% strength drop from its maximum resistance; (c) the first attainment of 95% of the maximum base-shear of the structure.

For precast-industrial structures, the conditions adopted were (a) widespread light damage corresponding to having attained 50% of the maximum shear strength in the panel-structure connection (i.e., at the yielding of the bolts or nuts); (b) at least one cladding panel reached the maximum strength of the panel-structure connection (i.e., failure of the bolt or opening of the channel lips).

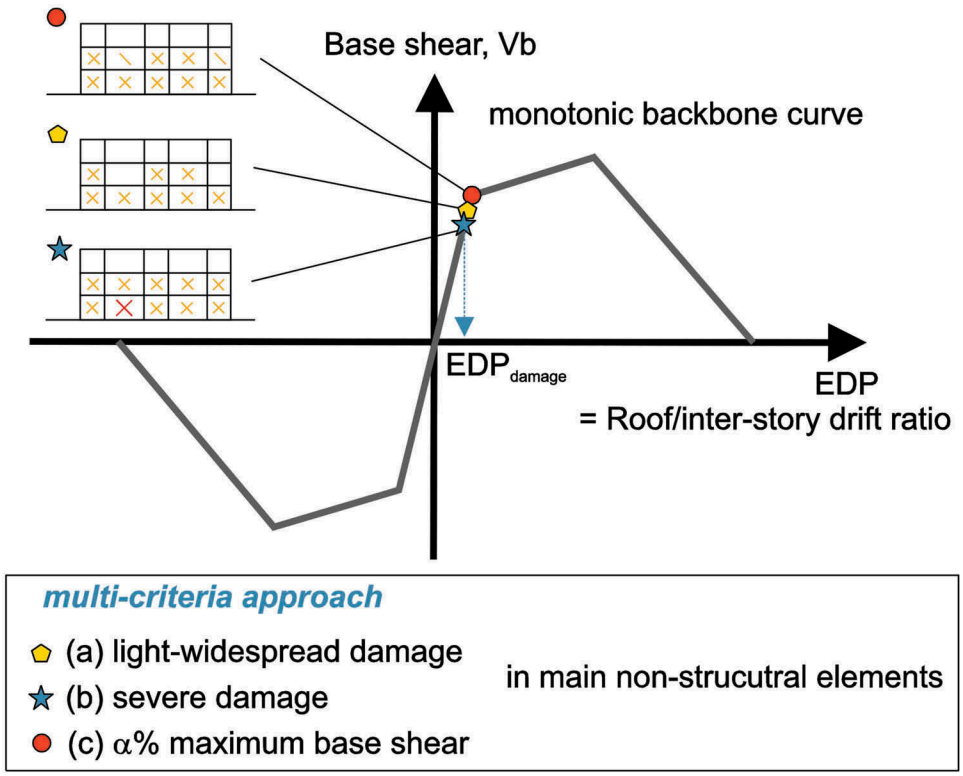

Figure 7. General definition for the usability-preventing damage failure criteria.

Finally, for steel structures, the criteria adopted were (a) widespread light damage (i.e., yielding inpanel-to-frame connection) in 50% of the cladding (sandwich) panels, in each horizontal direction; (b) at least one panel-to-frame connection reached its maximum strength; (c) having attained 95% of the maximum base-shear of the structure.

5. Seismic Hazard and Record Selection for Nonlinear Dynamic Analysis

Equation (1) requires hazard curves to compute the failure rates. As mentioned earlier, the design seismic actions in the Italian code (e.g., design spectra as those in Fig. 1, right) are based on PSHA. The results of the probabilistic hazard study that underlies the NTC (http://esse1-gis.mi.ingv.it/) are available for a grid of more than 10,000 locations over the whole country in terms of hazard curves for 5% damped (pseudo)spectral acceleration on A-type soil, for 11 natural vibration periods ranging from 0 s (PGA) to 2 s [Stucchi *et al.*, 2011]. The hazard curves, which are discretized at nine return periods ranging from 30 to 2475 years, are used to derive the UHS on rock on which the design spectra are based (an approximation of the UHS for other soil conditions is obtained by applying correction factors to the UHS for rock).

One could argue that these hazard curves could be sufficient to determine the failure rates. However, they are not suitable for that purpose, mainly because they are available at too few vibration periods and because those available are characterized by too tight a

range of return periods. Thus, hazard was computed ad-hoc at all sites and for the two soil classes, and for the spectral ordinates corresponding to the following first-mode vibration periods: $T_1 = \{0.15\text{s}, 0.5\text{s}, 1.0\text{s}, 1.5\text{s}, 2.0\text{s}\}$. For L'Aquila and Naples, hazard curves for $T_1 = 3.0\text{s}$ were also computed. All the hazard curves were calculated according to Eq. (4),

$$\lambda_{IM}(x) = \sum_{i=1}^{s} \nu_i \cdot \iint_{M,R} P[IM > x | M = w, R = z] \cdot f_{M,R,i}(w,z) \cdot dz \cdot dw \tag{4}$$

where $\nu_i,\ i = \{1, 2, \ldots, s\}$ is the rate of earthquakes above a minimum magnitude (M) for each of the s seismic source zones affecting the hazard at the site of interest; $f_{M,R,i}(w,z)$ is the joint probability density function of magnitude and source-to-site distance, (R), of the ith zone; and $P[IM > x | M = w, R = z]$ is the exceedance probability conditional to $\{M, R\}$ as provided by a ground-motion prediction equation (GMPE).

The source model of Meletti *et al.* [2008], which is used in Stucchi *et al.* [2011], was considered. It features the 36 seismic source zones depicted in Fig. 1 (left), and no background seismicity. The source characterization in terms of rates and magnitude distribution is that of Barani *et al.* [2009], and the GMPE selected for computing the hazard for spectral accelerations at periods shorter than 2.0 s is the one of Ambraseys *et al.* [1996]. For longer periods, needed for predicting the response of BI (i.e., base-isolated) structures, the GMPE of Akkar and Bommer [2010] was employed, given that the GMPE of Ambraseys *et al.* [1996] was not applicable. A uniform location distribution in each zone was assumed. All PSHA calculations have been carried out via OPENQUAKE [Monelli *et al.*, 2012].

The hazard curves were discretized at the ten IM values corresponding to the following return periods: $T_R = \{10, 50, 100, 250, 500, 1000, 2500, 5000, 10000, 100000\}$ years. No hazard curves for return periods longer than $T_R = 100000$ years were calculated to avoid large extrapolations. Fig. 8 shows the computed hazard curves for two spectral ordinates at the three sites of interest for both of the considered soil classes (A and C).

Note that, although the source model considered herein for hazard assessment lies at the basis of the hazard map used by the code, the latter is based on a logic tree, while only one branch is considered in this study. Therefore, the design accelerations of Fig. 1 (right)

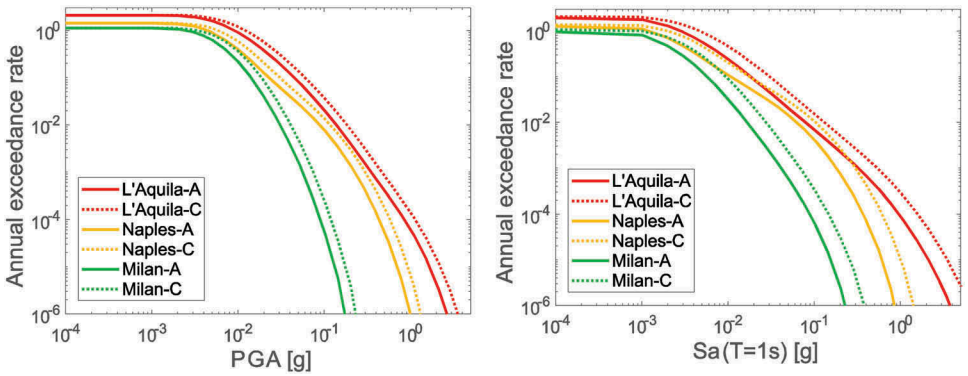

Figure 8. Hazard curves for two spectral ordinates and soil types computed for the considered three sites.

Table 2. Design PGA on A-type soil class for the damage and life-safety limit states according to the code and exceedance return period in the computed hazard curves.

	Life-safety design PGA [g]	T_R [years]	Damage PGA [g]	T_R [years]
L'Aquila	0.2607	479	0.104	54
Napoli	0.1668	439	0.06	49
Milano	0.0495	603	0.024	46

are expected to have a different return period according to the hazard curves of Fig. 8. Such a difference can be appreciated in Table 2 where, for the A-type soil PGAs used for life-safety and damage design, the return periods in the curves in Fig. 8 (left) are given. Generally, there is consistency between the return periods from the curves of this study and return periods from the code map.

Disaggregation of seismic hazard [e.g., Bazzurro and Cornell, 1999] was also carried out because, as will be discussed later, it is required for hazard-consistent record selection for nonlinear dynamic analysis. Disaggregation is the procedure, within the PSHA framework, used to determine the earthquake scenarios most likely being causative of the occurrence or exceedance of intensity equal to x. Before recalling the disaggregation equation, it may be worthwhile to rewrite the hazard integral as in Eq. (5).

$$\lambda_{IM}(x) = \sum_{i=1}^{s} v_i \cdot \iiint_{M,R,\varepsilon} I[IM>x|M=w,R=z,\varepsilon=e] \cdot f_{M,R,i}(m,r) \cdot f_{\varepsilon}(e) \cdot d\varepsilon \cdot dz \cdot dw \tag{5}$$

In the equation, $f_{\varepsilon}(e)$ is the PDF of ε, which is the standardized residual of a GMPE, calculated at the e value (the equation is written for GMPEs with ε independent of $\{M,R\}$). Once $\{M,R,\varepsilon\}$ are specified, $P[IM>x|M=w,R=z,\varepsilon=e]$ degenerates in the indicator function, $I[IM>x|M=w,R=z,\varepsilon=e]$, which equals 1 in the case of exceedance and 0 otherwise. At this point, it is possible to write Eq. (6), which is the equation that is used in hazard disaggregation for computing the PDF of $\{M,R,\varepsilon\}$ conditional to IM exceedance.

$$f_{M,R,\varepsilon|IM>x}(w,z,e) = \frac{\sum_{i=1}^{s} v_i \cdot I[IM>x|M=w,R=z,\varepsilon=e] \cdot f_{M,R,\varepsilon,i}(w,z,e)}{\lambda_{IM}(x)} \tag{6}$$

As an example, Fig. 9 presents the hazard disaggregation of $Sa(T=1.0\text{s})$, in terms of magnitude and distance and ε, for the three sites considered and the two IM values corresponding to $T_R = 475$ years and $T_R = 100,000$ years.

The disaggregation for L'Aquila at $T_R = 475$ years shows that the hazard is generally dominated by close events of relatively moderate magnitude, although earthquakes at large distances from the site provide non-negligible contributions. At large return periods, the magnitude most likely causative for the exceedance of the IM increases and the contributions are almost exclusively from small distances.

Note that disaggregation for L'Aquila is unimodal: the hazard is dominated by the source zone where the site is located (Fig. 1). This is not the case of Naples, for which the disaggregation shows a bimodal distribution with peaks for both low-magnitude short-distance earthquakes and high-magnitude long-distance earthquakes. The former set of earthquakes occurs in the zone around Naples, while the latter set are earthquakes

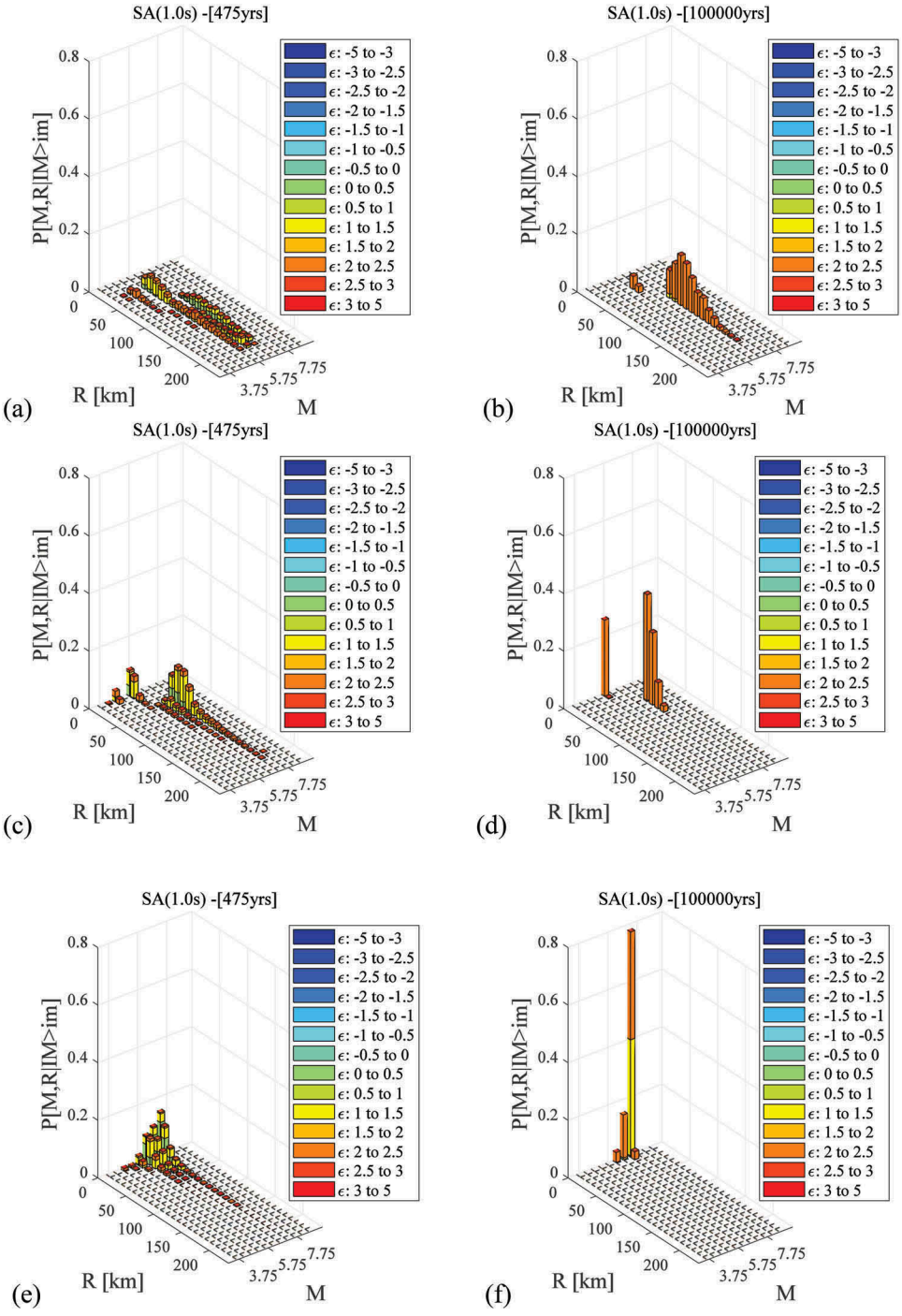

Figure 9. Magnitude and distance disaggregation of 475-year and 100,000-year return period spectral accelerations at 1.0 s, computed for soil A in the sites of Milan (a,b), Naples (c,d), and L'Aquila (e,f).

occurring along the southern Apennines mountains. Also, in the case of Naples, the disaggregation associated to the largest return period is less dispersed.

Finally, the disaggregation for Milan also shows a bimodal distribution with contributions only from far earthquakes. This is because Milan is outside any source zone; therefore, no nearby earthquakes can occur. The two modes correspond to earthquakes generated by the most relevant sources among those surrounding the site. For a more in-depth discussion about the shape of disaggregation distributions for Italian sites, the interested reader is referred to Iervolino *et al.* [2011].

5.1. *Record Selection*

Seismic input selection for nonlinear dynamic analysis of computer models was hazard-consistent at the state of the art, which means that records are selected consistent with hazard-based spectral shape and source features in terms of magnitude and distance. More precisely, the selection approach was based on the (exact) *conditional spectrum* (CS) method proposed by Lin *et al.* [2013], further enhanced to include a post-processing procedure that allows to ensure consistency of selected records with the magnitude and distance from disaggregation [Spillatura, 2018]. This method can implicitly account for ground-motion record characteristics other than spectral shape. Since the results of disaggregation change with return period, different sets of records were selected for different intensity levels.

For each site and each natural vibration (first-mode) period of interest, the adopted selection procedure can be summarized as follows: (a) carry out disaggregation conditional to $Sa(T_1) = x$, where x corresponds to the 10 values having exceedance return periods from 10 to 100,000 years at each of the three sites; (b) build the corresponding CS distribution for each x-value; (c) simulate an arbitrary number of response spectra, 20 herein, consistent with the CS defined at the previous step; (d) select 20 records that have spectra compatible with those simulated; (e) post-process the selected set substituting the records that are not disaggregation-consistent with other spectrally equivalent ground-motions with desired $\{M, R\}$. As an example, Fig. 10 shows the ten conditional spectra (mean and two percentiles) for the Milan (left) and L'Aquila (right) sites (soil C class), when the conditioning IM is $Sa(T = 1\text{s})$.

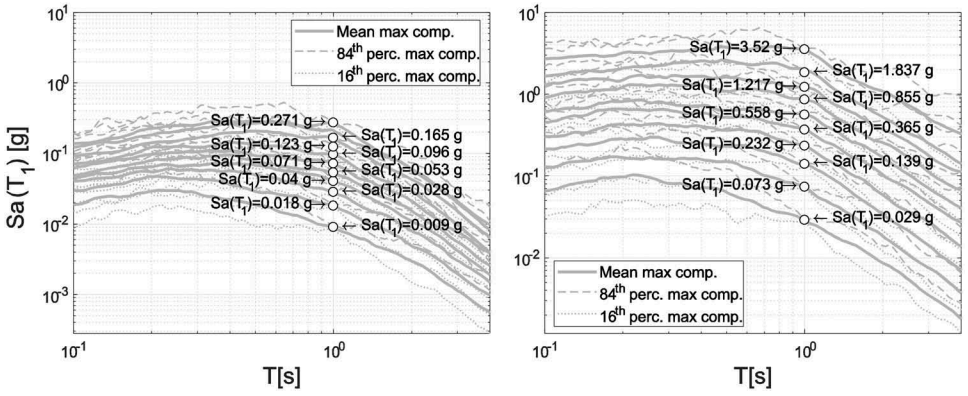

Figure 10. Conditional spectra (mean and two percentiles) referring to the Milan (left) and L'Aquila (right) sites for soil C class, when the conditioning IM is $Sa(T_1 = 1\text{s})$.

The selected records were extracted from the Italian accelerometric archive (http://itaca.mi.ingv.it/; Luzi *et al.* [2008]) and when no records with suitable spectral shape were available there, the algorithm searched for records in the NGAwest2 (http://peer.berkeley.edu/ngawest2/) database [Ancheta *et al.*, 2014].[7]

The record selection procedure resulted in 200 pairs of records for each combination of site, *Sa*, and soil conditions. Those 200 records are split in 10 sets (1 per stripe) of 20 horizontal ground-motions (pairs). Since the three-dimensional structural models required considerable computational effort, especially for the largest IM-levels causing severe nonlinear demands, the selected records have been processed to reduce their length. This has been done removing the parts of the signal outside the $\{t_{0.05\%}, t_{99.95\%}\}$ range, where $D_{99.90\%} = t_{99.95\%} - t_{0.05\%}$ is the 99.90% *significant duration* of the record [Dobry *et al.*, 1978]. Of course, synchronization of horizontal components after post-processing was kept. This procedure significantly reduced the analysis time, yet it was verified that it did not changed the computed seismic response in terms of the EDP of interest.

6. Results and Discussions

Before introducing the results, it must be recalled that Eq. (1) can be used for the computation of failure rates only for the values of $\lambda_{IM}(x)$ provided by hazard analysis; with the latter, as discussed, having a limit at $T_R = 100,000$ years. This, in principle, prevents to fully evaluate the failure rate. Therefore, it has been conservatively assumed that ground-motions with an IM larger than that corresponding to $T_R = 100,000$ years, $IM_{T_R^*}$, will certainly cause failure. This means that the failure rate has been conservatively approximated by Eq. (7).

$$\begin{aligned}\lambda_f &= \int_0^{IM_{T_R^*}} P[failure|IM = x] \cdot |d\lambda_{IM}(x)| + \int_{IM_{T_R^*}}^{+\infty} 1 \cdot |d\lambda_{IM}(x)| \\ &= \int_0^{IM_{T_R^*}} P[failure|IM = x] \cdot |d\lambda_{IM}(x)| + 10^{-5}\end{aligned} \tag{7}$$

When the first part of the integral is negligible with respect to 10^{-5}, Eq. (7) only allows to state that the annual failure is lower than 10^{-5}.

6.1. *Failure Rates*

Figures 11–14 give an overview of the annual failure rates associated with global collapse and usability-preventing damage for both soil conditions, C-type and A-type. The sites (from left to right) are ordered in terms of ascending hazard level, while the markers refer to the different structural types and configurations reported in Table 1. For each site, different vertical alignments of the markers help distinguish the various structural types. Failure rates equal to 10^{-5} correspond to cases for which the hazard beyond $IM_{T_R^*}$ dominates the risk integral, and 10^{-5} is an upper bound to the failure rate.

The figures show that, independently of the performance level and soil class considered, the seismic structural reliability tends to decrease as the hazard of the site increases. This trend holds despite the fact that the design actions have the same return period of

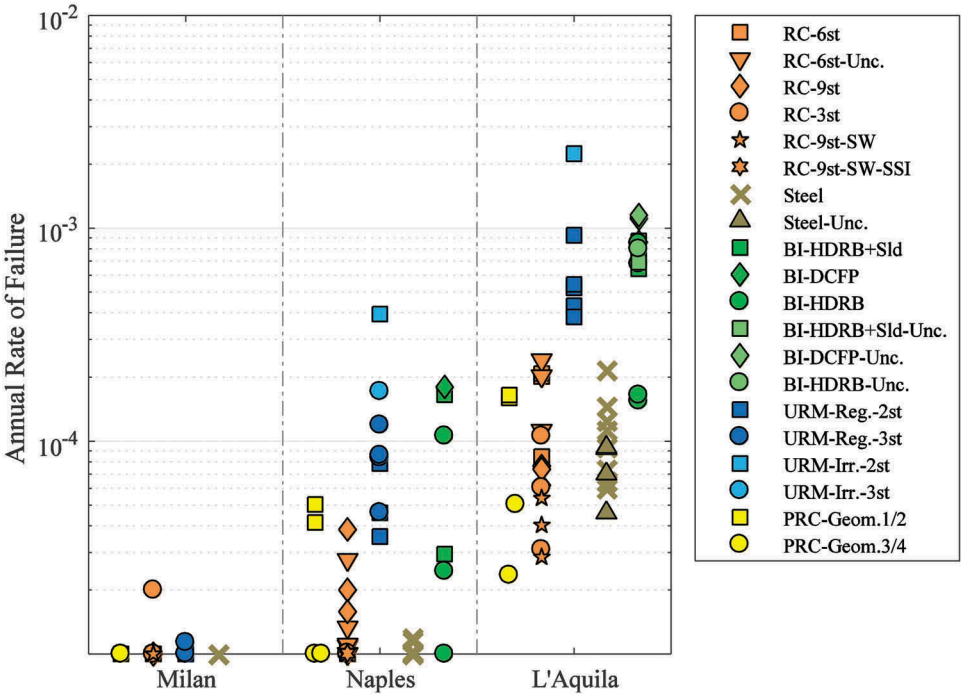

Figure 11. Global collapse failure rates (soil C-type).

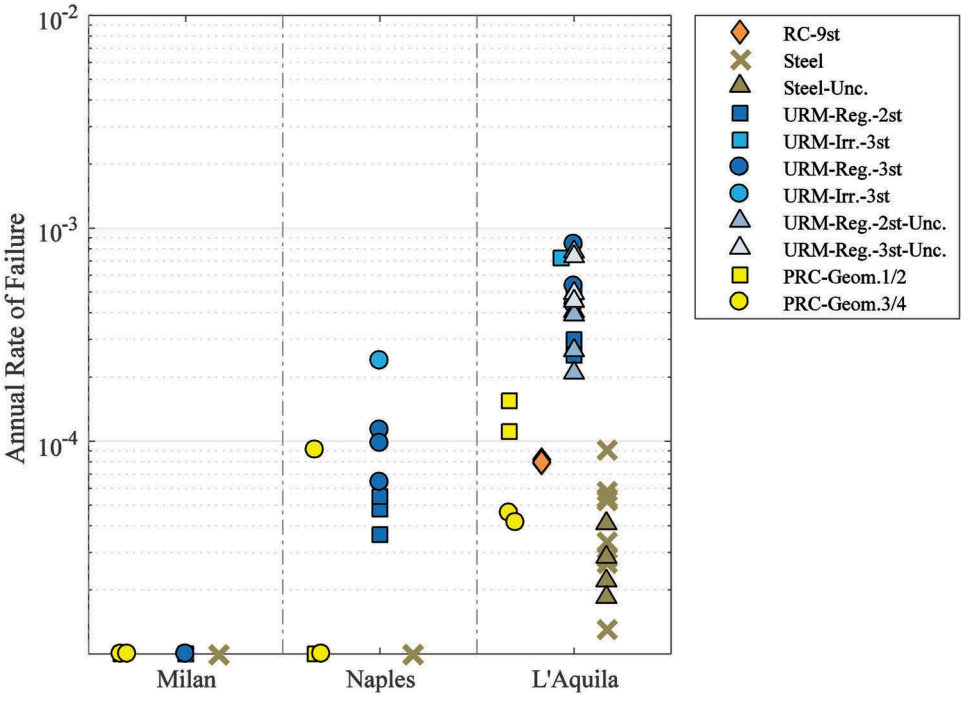

Figure12. Global collapse failure rates (soil A-type).

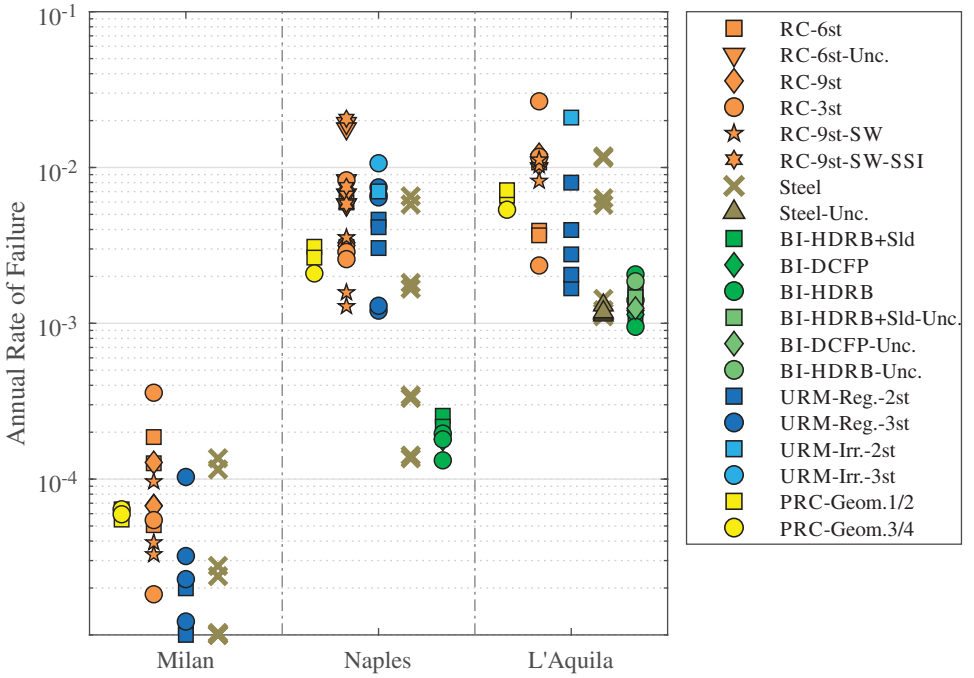

Figure 13. Usability-preventing damage failure rates (soil C-type).

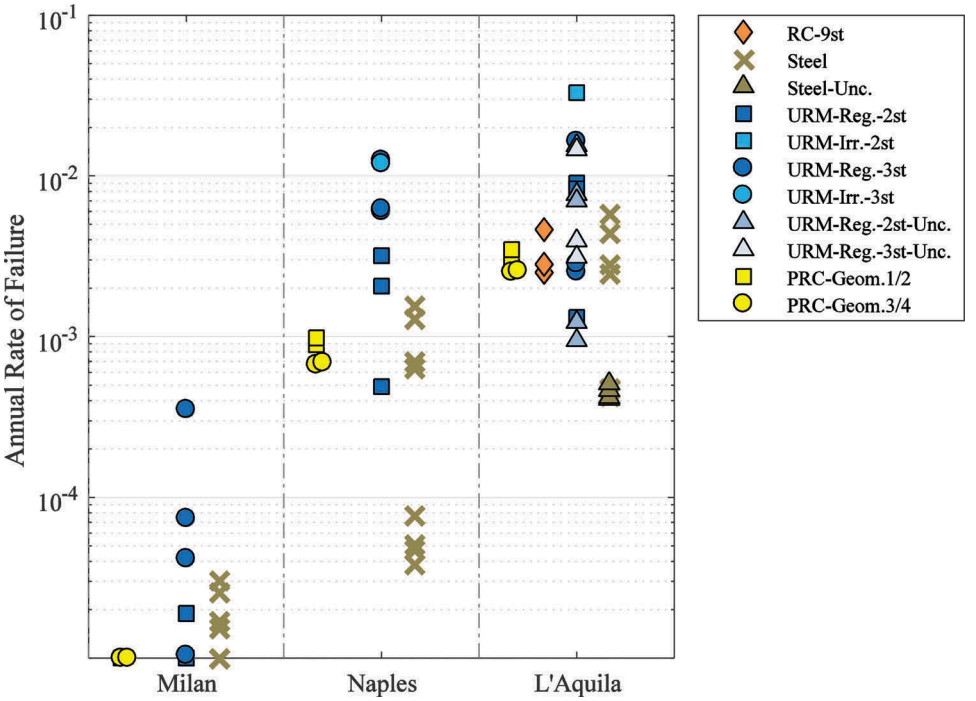

Figure 14. Usability-preventing damage failure rates (soil A-type).

exceedance, and other design choices, such as the behavior factor, are the same across structures designed at different sites. In particular, looking at global collapse at the less hazardous sites, for some site-structure combinations, the computed failure rates are so low that only an upper bound of 10^{-5} can be assigned. Conversely, the global collapse rate increases even by two orders of magnitude, in least at L'Aquila, that is the most hazardous site [see also Suzuki *et al.*, 2018, for a discussion].

It is interesting to note that in some cases, the failure rates are comparable to the exceedance rate of the design ground-motion acceleration, which is equal to 0.0021 when the return period is 475 years (life-safety) and to 0.02 when the return period is 50 years (damage). However, it is to recall that the failure conditions considered in this study are an arbitrary choice of the researchers involved in the RINTC project.

Although, as discussed later on, the comparison of failure rates among typologies requires some caution, when global collapse is considered, the comparatively less reliable structures tend to be the URM buildings. Moreover, the failure rates for usability-preventing damage show some general comparability among the structural typologies, except for BI structures. In fact, the analyses show global collapse failure rates comparable to, or larger than, those of the fixed-base structures. On the other hand, the failure rates for the usability-preventing damage are significantly lower than the others. This observation may possibly suggest that the BI structures, because of their more controlled behavior from design (i.e., of the isolation system), show a less (uncontrolled) margin against collapse, with respect to fixed-base structures. For this same reason, they show less risk with respect to the usability-preventing damage. Nevertheless, also modeling of the isolation system's failure may also play a non-negligible role in determining these conclusions; therefore, for in-depth understanding of these results, the interested reader is referred to Ragni *et al.* [2018].

Finally, for what concerns the effect of modeling uncertainty, it is observed that it generally tends to decrease the seismic reliability. However, in all investigated cases over all structural typologies, the rates that include modeling uncertainty vary mildly with respect to their counterparts where only record-to-record variability is accounted for (i.e., they are always within the same order of magnitude). Similar conclusions apply for the effect of SSI. Nevertheless, in discussing these conclusions, the limited number of cases analyzed for these effects and the modeling choices made must be kept in mind.

Tables 3 and 4 summarize the average failure rates computed per typology and per site (note that the values for RC structures include BF results) not considering SSI and Unc. cases.

In analyzing these tables, and possibly comparing the average rates among structural typologies, it must be emphasized that design and modeling, although carried out in a

Table 3. Average global collapse failure rates per structural typology and per site.

	C-type			A-type		
	Milan	Naples	L'Aquila	Milan	Naples	L'Aquila
URM	1.02E−05	1.15E−04	8.41E−04	1.00E−05	9.33E−05	5.11E−04
PRC	1.00E−05	2.80E−05	9.98E−05	1.00E−05	3.03E−05	8.84E−05
RC	1.08E−05	1.38E−05	8.56E−05	–	–	8.02E−05
S	1.00E−05	1.05E−05	1.12E−04	1.00E−05	1.00E−05	4.50E−05
BI	–	8.59E−05	6.93E−04	–	–	–

Table 4. Average usability-preventing damage failure rates per structural typology and per site.

	C-type			A-type		
	Milan	Naples	L'Aquila	Milan	Naples	L'Aquila
URM	3.02E−05	5.08E−03	6.56E−03	6.72E−05	6.07E−03	1.05E−02
PRC	6.06E−05	2.54E−03	6.01E−03	1.00E−05	8.08E−04	2.87E−03
RC	1.02E− 4	3.82E−03	1.03E−02	–	–	3.32E−03
S	4.29E−05	2.10E−03	5.04E−03	1.61E−05	5.52E−04	2.17E−03
BI	–	1.93E−04	1.41E−3	–	–	–

consistent manner as much as possible within the project this study refers to, reflect different choices and expertise of the research groups involved. Therefore, the main result is represented by the general trend of the rates and the within-typology variability of the rates with respect to the investigated structural configurations and design hazard. Any reliability comparison among typologies should be carried out always keeping in mind specific design and modeling choices as described in the typology-specific papers referenced in Sec. 3.[8]

7. Conclusions

This paper presented the main results of a 3-years research project targeted at estimating the seismic structural reliability of the most common code-conforming building typologies in Italy. The considered structures were designed for damage-limitation and life-safety for two soil conditions at three sites characterized by seismic hazard ranging from low-to-high in the country. The response of these structures was assessed via nonlinear dynamic analysis (in the form of multi-stripe analysis), carried out on three-dimensional models with state-of-the-art calibration. The results of reliability analysis are the annual rates of earthquakes able to cause structural failure, intended here as global collapse and usability preventing damage. The failure rates were evaluated in the performance-based earthquake engineering framework, that is combining the seismic fragility with the sites' hazard evaluated via probabilistic analysis. The uncertainty was accounted for in the hazard and in the record-to-record variability of structural response. For selected cases, soil-structure interaction and uncertainty in structural characteristics were also accounted for. The following results are worth to remark.

(1) Despite the homogeneity of design seismic actions and engineering choices, the seismic structural reliability tends to decrease with the seismic hazard of the sites. Regardless of typology and considered performance level, the failure rates tend to be larger, even by orders of magnitudes, for the buildings located at the most hazardous sites.
(2) For the less hazardous sites, the failure rates are so low that only an upper bound to the actual failure rate can be provided; i.e., $\lambda_f \leq 10^{-5}$. On the other hand, the failure rates of buildings at the most hazardous of the sites are, in some cases, comparable to the annual rate of exceedance of the design ground-motion intensity.
(3) Modeling uncertainty in structural characteristics and SSI appears, at least in the few considered cases, only to mildly change the failure rates if compared to the corresponding configurations that do not account for these factors.

These conclusions on failure rate trends notwithstanding, it should be noted that the failure criteria as well as the other design and modeling options considered in the study

carry a certain degree the arbitrary choices of the researchers involved. Hence, the absolute values of the failure rates and the reliability comparisons among typologies must be interpreted and used with due caution.

Notes

1 In fact, five sites were originally selected [see RINTC Workgroup, 2018], but three are sufficient to describe the core of the project's results.
2 In the framework considered, the annual failure rates, when sufficiently small, are numerically equivalent to the annual failure probabilities.
3 This is the case of structures for which the failure has to be verified by means of multiple EDPs.
4 The failure rates computed in this way are based on samples of structural response and, as such, they are subject to estimation uncertainty [e.g., Iervolino, 2017]. Moreover, the effect on the computed rate of different ways in which the integral in Eq. (1) is computed (approximated) also can have an effect. Both these issues are not directly addressed herein.
5 It was mentioned that the Italian code has extended similarities in design principles and procedures with Eurocode 8; however, the two codes have also significant differences. For example, the *damage-limitation* limit state in the EC8 corresponds to 95 years return period of exceedance of the design seismic actions. Because it is not possible to compare here the two codes for all structural typologies and configurations, the interested reader is referred to the typology-specific papers cited in this section for further details.
6 Not all the irregular configurations analyzed in the project were included in the results discussed herein. A complete description of the investigated cases can be found in RINTC Workgroup [2018].
7 Note that to be consistent with the IM adopted by the GMPE of Ambraseys *et al.* [1996], which is the maximum between the horizontal components, the matching of the CS is in term of this IM. Conversely, for those cases where the GMPE of Akkar and Bommer [2010] was considered, the CS matching was carried out using the geometric mean of the two horizontal components.
8 In Iervolino *et al.* [2017] and Iervolino [2018], where preliminary results were commented, it was concluded that the failure rates were not uniform across different typologies designed for the same site and same limit state. This was mainly because of precast structures and some irregular URM configurations. In the former case, the failure rates were much higher than any other structure, because of the design criterion of beam-to-column connection, which has been revised toward a more state-of-the-art design approach reducing the failure rates. In the latter case, the irregular URM configuration in question is not included in the results herein as already mentioned.

Acknowledgments

The study presented in this article was developed within the activities of the ReLUIS-DPC and EUCENTRE-DPC 2014–2018 research programs, funded by the *Presidenza del Consiglio dei Ministri—Dipartimento della Protezione Civile* (DPC). Note that the opinions and conclusions presented by the authors do not necessarily reflect those of the funding entity. Finally, the authors acknowledge the comments by Dimitrios Vamvatsikos (*National Technical University of Athens*, Greece) and an anonymous reviewer.

References

Akkar, S. and Bommer, J. J. [2010] "Empirical equations for the prediction of PGA, PGV, and spectral accelerations in Europe, the mediterranean region, and the middle east," *Seismological Research Letters* **81**, 195–206. doi:10.1785/gssrl.81.2.195.

Ambraseys, N. N., Simpson, K. U. and Bommer, J. J. [1996] "Prediction of horizontal response spectra in Europe," *Earthquake Engineering & Structural Dynamics* **25**, 371–400. doi:10.1002/(SICI)1096-9845(199604)25:4<371::AID-EQE550>3.0.CO;2-A.

Ancheta, T. D., Darragh, R. B., Stewart, J. P., Seyhan, E., Silva, W. J., Chiou, B. S. J., Wooddell, K. E., Graves, R. V., Kottke, A. R., Boore, D. M., Kishida, T. and Donahue, J. L. [2014] "NGA-West2 database," *Earthquake Spectra* **30**, 989–1005. doi:10.1193/070913EQS197M.

Barani, S., Spallarossa, D. and Bazzurro, P. [2009] "Disaggregation of probabilistic ground-motion hazard in Italy," *Bulletin of the Seismological Society of America* **99**, 2638–2661. doi:10.1785/0120080348.

Bazzurro, P. and Cornell, C. A. [1999] "Disaggregation of seismic hazard," *Bulletin of the Seismological Society of America* **89**, 501–520.

C.E.N. [2004] *Eurocode Eurocode 8: Design of Structures for Earthquake Resistance: Part 1: General Rules, Seismic Actions and Rules for Buildings*, European Committee for Standardization, Bruxelles, Belgium.

Camata, G., Celano, F., De Risi, M. T., Franchin, P., Magliulo, G., Manfredi, V., Masi, A., Mollaioli, F., Noto, F., Riccci, P., Spacone, E. and Terrenzi, M. [2017] "RINTC project: nonlinear dynamic analyses of Italian code-conforming reinforced concrete buildings for risk of collapse assessment," *Proc. of COMPDYN 2017 – 6th ECCOMAS Thematic Conference on Computational Methods in Structural Dynamics and Earth-quake Engineering*, Rhodes Island, Greece.

Camilletti, D., Cattari, S., Lagomarsino, S., Bonaldo, D., Guidi, G., Bracchi, S. … Rota, M. [2017] "RINTC project: nonlinear dynamic analyses of Italian code-conforming URM buildings for collapse risk assessment," *Proc. of COMPDYN 2017 – 6th ECCOMAS Thematic Conference on Computational Methods in Structural Dynamics and Earth-quake Engineering*, Rhodes Island, Greece.

Cardone, D., Conte, N., Dall'Asta, A., Di Cesare, A., Flora, A., Leccese, G., Mossucca, A., Micozzi, F., Ponzo, F. C. and Ragni, L. [2017] "RINTC project: nonlinear analyses of Italian code-conforming base-isolated buildings for risk of collapse assessment," *Proc. of COMPDYN 2017 – 6th ECCOMAS Thematic Conference on Computational Methods in Structural Dynamics and Earth-quake Engineering*, Rhodes Island, Greece.

Cattari, S., Camilletti, D., Lagomarsino, S., Bracchi, S., Rota, M. and Penna, A. [2018] "Masonry Italian code-conforming buildings. Part 2: nonlinear modelling and time-historey analysis," *Journal of Earthquake Engineering*. in press. doi:10.1080/13632469.2018.1541030.

Cornell, C. A. [1968] "Engineering seismic risk analysis," *Bulletin of the Seismological Society of America* **58**, 1583–1606.

Cornell, C. A. and Krawinkler, H. [2000] "progress and challenges in seismic performance assessment," *PEER Center News* **3**.

CS.LL.PP.. [2008] "Norme tecniche per le costruzioni," *Gazzetta Ufficiale della Repubblica Italiana* **29** (In Italian.).

CS.LL.PP.. [2018] "Aggiornamento delle norme tecniche per le costruzioni," *Gazzetta Ufficiale della Repubblica Italiana* **42** (In Italian.).

Dobry, R., Idriss, I. M. and Ng, E. [1978] "Duration characteristics of horizontal components of strong-motion earthquake records," *Bulletin of the Seismological Society of America* **68**, 1487–1520.

Ercolino, M., Cimmino, M., Magliulo, G., Bellotti, D. and Nascimbene, R. [2017] "RINTC project: nonlinear analyses of Italian code conforming precast R/C industrial buildings for risk of collapse assessment," *Proc. of COMPDYN 2017 – 6th ECCOMAS Thematic Conference on Computational Methods in Structural Dynamics and Earth-quake Engineering*, Rhodes Island, Greece.

Franchin, P., Mollaioli, F. and Noto, F. [2017] "RINTC project: influence of structure-related uncertainties on the risk of collapse of Italian code-conforming reinforced concrete buildings," *Proc. of COMPDYN 2017 – 6th ECCOMAS Thematic Conference on Computational Methods in Structural Dynamics and Earth-quake Engineering*, Rhodes Island, Greece.

Franchin, P., Ragni, L., Rota, M. and Zona, A. [2018] "Modelling uncertainties of Italian code-conforming structures for the purpose of seismic response analysis," *Journal of Earthquake Engineering*. in press. doi:10.1080/13632469.2018.1527262.

Iervolino, I. [2017] "Assessing uncertainty in estimation of seismic response for PBEE," *Earthquake Engineering and Structural Dynamics* **46**, 1711–1723. doi:10.1002/eqe.2883.

Iervolino, I. [2018] "What seismic risk do we design for when we design buildings?," *Geotechnical, Geological and Earthquake Engineering* **46**, 583–602.

Iervolino, I., Chioccarelli, E. and Convertito, V. [2011] "Engineering design earthquakes from multimodal hazard disaggregation," *Soil Dynamics and Earthquake Engineering* **31**, 1212–1231. doi:10.1016/j.soildyn.2011.05.001.

Iervolino, I., Spillatura, A. and Bazzurro, P. [2017] "RINTC project-assessing the (implicit) seismic risk of code-conforming structures in Italy," *Proc. of COMPDYN 2017 – 6th ECCOMAS Thematic Conference on Computational Methods in Structural Dynamics and Earthquake Engineering*, Rhodes Island, Greece.

Jalayer, F. [2003] "*Direct Probabilistic seismic analysis: implementing nonlinear dynamic assessment*," Ph.D. thesis, Department of Civil and Environmental Engineering, Stanford University, Stanford, CA, USA.

Lagomarsino, S., Penna, A., Galasco, A. and Cattari, S. [2013] "TREMURI program: an equivalent frame model for the nonlinear seismic analysis of masonry buildings," *Engineering Structures* **56**, 1787–1799. doi:10.1016/j.engstruct.2013.08.002.

Lin, T., Haselton, C. B. and Baker, J. W. [2013] "Conditional spectrum-based ground-motion selection. Part I: hazard consistency for risk-based assessments," *Earthquake Engineering and Structural Dynamics* **42**, 1847–1865. doi:10.1002/eqe.2301.

Luzi, L., Hailemikael, S., Bindi, D., Pacor, F., Mele, F. and Sabetta, F. [2008] "ITACA (ITalian ACcelerometric Archive): a web portal for the dissemination of Italian strong-motion data," *Seismological Research Letters* **79**, 716–722. doi:10.1785/gssrl.79.5.716.

Magliulo, G., Bellotti, D., Cimmino, M. and Nascimbene, R. [2018] "Modeling and seismic response analysis of RC precast Italian code-conforming buildings," *Journal of Earthquake Engineering* 1–28. in press doi:10.1080/13632469.2018.1531093.

Manzini, C.F., Magenes, G., Penna, A., da Porto, F., Camilletti, D., Cattari, S., and Lagomarsino, S. [2018] "Masonry Italian code-conforming buildings: part 1: case studies and design methods," *Journal of Earthquake Engineering*. in press. doi: 10.1080/13632469.2018.1532358.

Mazzoni, S., McKenna, F., Scott, M. H. and Fenves, G. L. [2006] *The open system for earthquake engineering simulation (OpenSEES) user command-language manual*, Pacific Earthuquake Engineering Research Center, Berkeley, CA, USA. (available online at http://opensees.berkeley.edu).

McGuire, R. K. [2004] *Analysis of Seismic Hazard and Risk*, EERI Monograph, Earhtquake Engineering research Center, Oakland, CA, USA.

Meletti, C., Galadini, F., Valensise, G., Stucchi, M., Basili, R., Barba, S., Vannucci, G. and Boschi, E. [2008] "A seismic source zone model for the seismic hazard assessment of the Italian territory," *Tectonophysics* **450**, 85–108. doi:10.1016/j.tecto.2008.01.003.

Monelli, D., Pagani, M., Weatherill, G., Silva, V. and Crowley, H. [2012] "the hazard component of openquake: the calculation engine of the global earthquake model," *Proc. of 15WCEE – 15th World Conference on Earthquake Engineering*, Lisbon, Portugal.

Ragni, L., Cardone, D., Conte, N., Dall'Asta, A., Di Cesare, A., Flora, A., Leccese, G., Micozzi, F. and Ponzo, F. C. [2018] "Modeling and seismic response analysis of Italian code-conforming base-isolated buildings," *Journal of Earthquake Engineering* 1–33. in press. doi:10.1080/13632469.2018.1527263.

Ricci, P., Manfredi, V., Noto, F., Terrenzi, M., Celano, F., De Risi, M. T., Camata, G., Franchin, P., Magliulo, G., Masi, A., Mollaioli, F., Spacone, E., and Verderame, G. M. [2018] "Modelling and seismic response analysis of Italian codeconforming reinforced concrete buildings," *Journal of Earthquake Engineering*. in press. doi:10.1080/13632469.2018.1527733.

RINTC Workgroup [2018] *Results of the 2015-2017 implicit seismic risk of code-conforming structures in Italy (RINTC) project*, ReLUIS report, Rete dei Laboratori Universitari di Ingegneria Sismica, Naples, Italy. (available online at https://goo.gl/j8H7MV).

Scozzese, F., Terracciano, G., Zona, A., Della Corte, G., Dall'Asta, A. and Landolfo, R. [2017] "RINTC project: nonlinear dynamic analyses of Italian code-conforming steel single-story buildings for collapse risk assessment," *Proc. of COMPDYN 2017 – 6th ECCOMAS Thematic*

Conference on Computational Methods in Structural Dynamics and Earth-quake Engineering, Rhodes Island, Greece.

Scozzese, F., Terracciano, G., Zona, A., Della Corte, G., Dall'Asta, A. and Landolfo, R. [2018] "Modelling and seismic response analysis of Italian code-conforming single-storey steel buildings," *Journal of Earthquake Engineering* 1–30. in press doi:10.1080/13632469.2018.1528913.

Shome, N. and Cornell, C. A. [2000] "Structural seismic demand analysis: consideration of 'Collapse'," *Proc. of 8th ASCE Specialty Conference on Probabilistic Mechanics and Structural Reliability*. South Bend, Indiana, USA.

Spillatura, A. [2018] "From record selection to risk targeted spectra for risk-based assessment and design," Ph.D. Thesis, Dipartimento di Costruzioni e Infrastrutture, Istituto Universitario degli Studi Superiori (IUSS), Pavia, Italy.

Stucchi, M., Meletti, C., Montaldo, V., Crowley, H., Calvi, G. M. and Boschi, E. [2011] "Seismic hazard assessment (2003–2009) for the Italian building code," *Bulletin of Seismological Society of America* **101**, 1885–1911. doi:10.1785/0120100130.

Suzuki, A., Baltzopoulos, G. and Iervolino, I., and the RINTC WP4 Workgroup [2018] "A look at the seismic risk of italian code-conforming rc buildings", *Proc. of 16ECEE – 16th European Conference on Earthquake Engineering*, Thessaloniki, Greece.